
Learning Continuous Exponential Families Beyond Gaussian

Christopher X. Ren¹ Sidhant Misra² Marc Vuffray² Andrey Y. Lokhov²

Abstract

We address the problem of learning of continuous exponential family distributions with unbounded support. While a lot of progress has been made on learning of Gaussian graphical models, we are still lacking scalable algorithms for reconstructing general continuous exponential families modeling higher-order moments of the data beyond the mean and the covariance. Here, we introduce a computationally efficient method for learning continuous graphical models based on the Interaction Screening approach. Through a series of numerical experiments, we show that our estimator maintains similar requirements in terms of accuracy and sample complexity compared to alternative approaches such as maximization of conditional likelihood, while considerably improving upon the algorithm’s run-time.

1. Introduction

An exponential family is a general parametric set of probability distributions that are capable of capturing any positive probability measure (Koopman, 1936). Graphical models that aim to model conditional dependencies of high-dimensional probability distributions with discrete or continuous variables are commonly expressed in the exponential family form (Wainwright et al., 2008). Exponential family distributions are typically characterized by the energy function which specifies the sufficient statistic of the distribution, the associated parameters, and the graph structure of the underlying graphical model:

$$P(X) = \frac{1}{Z} \exp[E(X)], \quad (1)$$

where X denotes the set of random variables, $E(X)$ is the energy function, and Z is the normalization factor known as

¹Intelligence and Space Research Division, Los Alamos National Laboratory, USA ²Theoretical Division, Los Alamos National Laboratory, USA. Correspondence to: <cren@lanl.gov>, <sidhant@lanl.gov>, <vuffray@lanl.gov>, <lokhov@lanl.gov>.

the partition function. The energy function takes the general form

$$E(X) = - \sum_{m \in \mathcal{M}} \theta_m f_m(X_m), \quad (2)$$

where $\{f_m, m \in \mathcal{M}\}$, for some set \mathcal{M} , is a collection of basis functions each acting upon subsets of variables X_m . These basis functions are often referred to as the sufficient statistic of the model. The parameters $\theta_m \in \mathbb{R}$ specify a particular model within this family.

Perhaps the most famous continuous and unbounded exponential family is the multivariate Normal distribution with mean μ and covariance Σ . When defined on a p -dimensional graph $G = (V, E)$ with $|V| = p$, the energy function of a Gaussian Graphical Model (GGM) can be expressed as a quadratic function

$$E(X) = - \frac{1}{2} \sum_{i \in V} \theta_{ii} (x_i - \mu_i)^2 - \sum_{(i,j) \in E} \theta_{ij} (x_i - \mu_i)(x_j - \mu_j), \quad (3)$$

where μ_i denotes the mean of the variable x_i , and θ_{ij} are elements of the *precision matrix* Θ whose support is determined by the sparsity pattern of the graph G . GGMs have a special property that Θ is equal to the inverse of the covariance matrix Σ , meaning that $(\Sigma^{-1})_{ij} = 0$ for all $(i, j) \notin E$. GGMs are frequently used in applications where the random variables arise from sums of independent contributions and hence are well approximated by a multivariate Normal distribution due to the central limit theorem. However, numerous applications in natural sciences and artificial systems generate data with statistics that strongly deviate from Gaussian distributions, where higher-order moments are important (Banfield & Raftery, 1993). Examples of such non-Gaussian statistics include turbulent flows (Li & Meneveau, 2005), scattered waves (Jakeman & Tough, 1988), cosmic microwave background temperature (Kogut et al., 1996), diffusion of biomacromolecules (Ghosh et al., 2016), gene expression and bioinformatics (Ji et al., 2005), atmospheric data (Perron & Sura, 2013) and cloud data (Sengupta et al., 2016) available through remote-sensing imagery, modeling of color image pixels in the RGB space (Bouguila et al., 2004), and non-negative matrix factorization in recorded music (Hoffman et al., 2010). Motivated

by many applications which aim to explicitly model higher-order moments present in the data, it is natural to consider a generalization of GGMs consisting of adding higher-order sufficient statistics to the energy function. An example of such a generalization is a graphical model that models moments up to four:

$$E(X) = - \sum_i \theta_i x_i - \sum_{ij} \theta_{ij} x_i x_j - \sum_{ijk} \theta_{ijk} x_i x_j x_k - \sum_{ijkl} \theta_{ijkl} x_i x_j x_k x_l. \quad (4)$$

More generally, we can write the energy function with sufficient statistics f_m consisting of monomials acting upon subsets of variables X_m . In the example (4) above, \mathcal{M} is the set of multi-indices of size at most four and if $m = ijk$ we would have $f_m(X_m) = x_i x_j x_k$. The decomposition structure of the energy function can be conveniently represented as a *factor graph* with the elements θ_m acting as hyperedges or factors, see Fig. 1 for an example of how the different multi-body terms entering in the energy function on four variables are drawn.

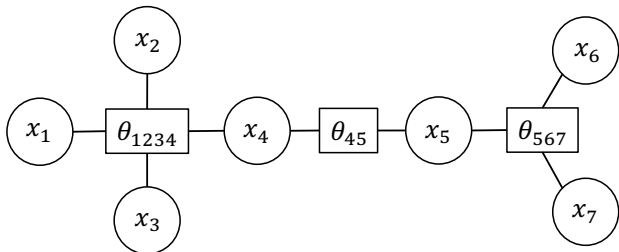


Figure 1. Example of a factor graph representation of the energy function of the type (4). For this example, the energy function reads $E(X) = -\theta_{45}x_4x_5 - \theta_{567}x_5x_6x_7 - \theta_{1234}x_1x_2x_3x_4$.

In this representation, the sparsity pattern of the array $\Theta = \{\theta_m, m \in \mathcal{M}\}$ provides interpretable structural information on the conditional dependencies between variables through the separation property of Markov Random Fields (MRFs). Given the rich structural information contained in the array of parameters, it is of interest to develop algorithms for reconstructing Θ and the underlying hypergraph from data. We consider the following learning problem.

Definition 1 (Learning Problem). *Given n i.i.d. samples $\{X^{(k)}\}_{k=1, \dots, n}$ drawn from an unknown probability measure (1) with the general energy function (2), estimate the parameter array Θ .*

If Θ is learned to a sufficient accuracy, a thresholded version of Θ will uncover the underlying hypergraph, and hence the structure of the conditional dependencies through the respective sparsity pattern. In the remainder of the paper, we assume that Θ is chosen in such a way that the distribution (1) is correctly defined.

Many efficient algorithms of different types are known for learning Gaussian graphical models (Meinshausen & Bühlmann, 2006; Tibshirani, 1996; Yuan & Lin, 2007; d’Aspremont et al., 2008; Ravikumar et al., 2009; Anandkumar et al., 2012; Cai et al., 2011; 2016), including polynomial-time algorithms achieving information-theoretic bounds in terms of sampling complexity for general GGMs (Misra et al., 2020) and important sub-classes of GGMs (Kelner et al., 2020). In comparison, scalable methods for learning general continuous exponential family distributions beyond Gaussian are still lacking. Unlike the Gaussian setting, the maximum likelihood estimator is computationally intractable for general continuous graphical models: the computation of the normalization factor

$$Z = \int_{-\infty}^{+\infty} \dots \int_{-\infty}^{+\infty} \left(\prod_{i=1}^N dx_i \right) \exp [E(X)] \quad (5)$$

results in a hard high-dimensional integration problem (Koutis, 2003).

A popular approach to the learning of high-dimensional distributions for which the maximum likelihood is intractable consists of using a pseudo-likelihood method that consistently recovers the model in polynomial time (Besag, 1975). The pseudo-likelihood approach is based on conditional likelihood maximization, and has been previously used for Gaussian distributions (Meinshausen & Bühlmann, 2006), discrete graphical models (Ravikumar et al., 2010; Klivans & Meka, 2017; Likhov et al., 2018), continuous generalized linear models (Yang et al., 2015; 2018), MRFs with pairwise potentials (Tansey et al., 2015; Yuan et al., 2016; Suggala et al., 2017), and mixed graphical models (Lee & Hastie, 2015). However, as we show in this work, the application of pseudo-likelihood to the challenging case of continuous distributions with unbounded support is hindered by the necessity of numerical computation of local normalization factors, rendering this estimation method impractical even for small number of random variables.

In practice, non-Gaussian statistics is often studied using other specific families of parametrized distributions, such as Beta, Dirichlet, Gamma, and Poisson distributions (Ma, 2011), or various mixture models (Titterton et al., 1985), for which tailored learning methods have been developed. Existing related works in the estimation of multivariate distributions that generalize Gaussian include semi-parametric methods, such as non-paranormal (Liu et al., 2009; Lafferty et al., 2012), Gaussian copula models for a certain choice of copula functions (Dobra et al., 2011; Liu et al., 2012), or rank-based estimators (Xue et al., 2012) which use transformations that “Gaussianize” the data, and then fit GGMs to estimate model structure. Other approaches include score matching for reproducing kernel Hilbert space parametrization (Sun et al., 2015), or a transport maps based approach

shown in (Morrison et al., 2017) which uses parametrization with Hermite polynomials.

In this work, we propose a general computationally efficient estimator for learning general continuous graphical models of the type (2). Our method is based on the *Interaction Screening* method introduced in (Vuffray et al., 2016) for pairwise graphical models over binary variables, and recently generalized to discrete graphical models with arbitrary degree of interactions and alphabet in (Vuffray et al., 2020) with improved sample-complexity on all existing methods. Unlike pseudo-likelihood, the Interaction Screening estimator does not include a normalization factor, and can be generalized to the case of noisy or corrupted data (Goel et al., 2019). In a recent work (Shah et al., 2020), the Interaction Screening method has been adapted to the setting of continuous graphical models, however this analysis was restricted to distributions with pairwise interactions, and more importantly to distributions with bounded support. Indeed, as we explain later in this paper, the vanilla Interaction Screening estimator introduced in (Vuffray et al., 2020) does not apply to continuous distributions with unbounded support. Here, we suggest a regularization of the Interaction Screening estimator that ensures that the estimator is well-behaved in the setting of general continuous exponential families with non-pairwise energy functions and unbounded support. We empirically show that this new *Interaction Screening Objective for Distributions with Unbounded Support (ISODUS)* estimator maintains similar requirements in terms of accuracy and sample complexity compared to pseudo-likelihood, while avoiding the numerical evaluation of a large number (order pn) of integrals at every step of the learning procedure, hence significantly improving upon pseudo-likelihood’s run-time.

2. Algorithms

First, we present the benchmark algorithm based on the Pseudo-Likelihood approach (Besag, 1975), and discuss challenges associated with the optimization for non-Gaussian graphical models. Then, we introduce our new ISODUS estimator based on the Interaction Screening principle (Vuffray et al., 2020).

2.1. Pseudo-likelihood

To introduce the pseudo-likelihood estimator, we first define the conditional distribution for a single variable x_i . For $i \in \{1, \dots, p\}$, let $\mathcal{M}_i \subseteq \mathcal{M}$ denote the set of monomials acting upon subsets X_m that contain the variable x_i . Let $E_i(X)$ denote the terms in $E(X)$ that participate in \mathcal{M}_i :

$$E_i(X) = - \sum_{m \in \mathcal{M}_i} \theta_m f_m(X_m). \quad (6)$$

Then, the conditional distribution of x_i reads

$$P(x_i | X_{\setminus i}) = \frac{1}{Z_i} \exp [E_i(X)], \quad (7)$$

where $X_{\setminus i}$ denotes the set of variables $\{x_i\}_{i \in V}$ with x_i removed from the set. For the example introduced in Eq. (4), the conditional distribution is

$$P(x_i | X_{\setminus i}) = \frac{1}{Z_i} \exp \left(- \theta_i x_i - \sum_j \theta_{ij} x_i x_j - \sum_{jk} \theta_{ijk} x_i x_j x_k - \sum_{jkl} \theta_{ijkl} x_i x_j x_k x_l \right).$$

The normalization factor, which we refer to as the local partition function, cannot be explicitly computed in general, and is given by a one-dimensional integral:

$$Z_i = Z_i(X_{\setminus i}) = \int_{-\infty}^{+\infty} dx_i \exp [E_i(x_i, X_{\setminus i})], \quad (8)$$

where notation $E_i(x_i, X_{\setminus i})$ implies that variables $X_{\setminus i}$ are fixed in this expression. Notice that the value of the normalization constant Z_i depends on the model parameters Θ_i , where Θ_i denote components of the array Θ that appear in $E_i(X)$. Let

$$\langle \cdot \rangle = \frac{1}{n} \sum_{k=1}^n (\cdot) \quad (9)$$

denote the empirical average over the samples $X^k_{k=1, \dots, n}$. The pseudo-likelihood approach aims to maximize the logarithm of the conditional distribution (7) as defined next.

Definition 2 (Pseudo-Likelihood Estimator). *The Pseudo-Likelihood estimator is defined as a series of independent local optimization problems over p nodes:*

$$\hat{\Theta}_i^{PL} = \operatorname{argmin}_{\Theta_i} - \langle \log P(x_i | X_{\setminus i}) \rangle \quad (10)$$

$$= \operatorname{argmin}_{\Theta_i} \langle -E_i(X) + \log Z_i \rangle. \quad (11)$$

Notice that due to the local form of the estimator (11), each component of the symmetric array Θ is estimated independently from each node’s neighborhood. As is common in local node-wise regressions, a single final estimate of the parameter is obtained by a consensus average of independent local estimates. A typical choice of the symmetrization procedure that has been analyzed in learning of discrete graphical models (Vuffray et al., 2020) consists of taking the arithmetic average of couplings estimated from different neighborhoods. In this work, we use the geometric mean to produce the final estimate of the components of Θ , following the arguments in (Misra et al., 2020) that showed that this choice of symmetrization is optimal for Gaussian graphical models. For instance, the final estimate for a pairwise coupling $\hat{\theta}_{ij}^{PL}$ will be given by $\sqrt{\hat{\theta}_{ij}^{PL} \hat{\theta}_{ji}^{PL}}$, the geometric

mean of couplings estimated from regressions based on the neighborhoods of i and j .

The minimization in (11) can be done by gradient descent, where at each iteration one needs to re-evaluate integrals of the type (8) by means of numerical integration, which can be costly if the integral needs to be computed to a high degree of precision. In the special case of Gaussian graphical models, Z_i can be computed explicitly, $Z_i = \sqrt{\theta_{ii}/\pi}$, and hence numerical integration is not required. In this local form, the pseudo-likelihood estimator is intimately connected to a node-wise regression approach introduced and analyzed for GGMs in (Meinshausen & Bühlmann, 2006), which reduces to a simple least-squares regression problem upon a simple change of variables.

2.2. Interaction Screening

The Interaction Screening estimator has been first introduced for Ising models in (Vuffray et al., 2016), and recently generalized to the case of arbitrary discrete graphical models with multi-body interactions in (Vuffray et al., 2020) where the Generalized Interaction Screening Objective (GISO) was introduced. In the case of general continuous distributions considered here, the Interaction Screening approach becomes particularly appealing due to its simple functional form that allows one to avoid the estimation of the local normalization factor Z_i . However, the GISO introduced in (Vuffray et al., 2020) does not directly apply to distributions with unbounded support. This is because first, the so-called centered basis functions that are required to construct the GISO may not exist due to diverging integrals. Second, even when the GISO can be constructed, all its moments may not be finite leading to poor scaling of its sample complexity.

To alleviate these issues, we propose a modified estimator based on the GISO that is suitable for general distributions. The key idea is the introduction of a *multiplicative regularizing distribution* (MRD) to make the GISO well behaved. For simplicity we choose the MRD in factorized form:

$$R(X) = \prod_{i=1}^p R_i(x_i), \quad (12)$$

where $R_i(x_i)$ is a probability distribution over variable x_i . For each basis term $f_m(X_m)$ in the energy function (2) and each variable x_i , we can now define the *local centering function* $g_{im}(X_m)$, centered with respect to the MRD as:

$$g_{im}(X_m) = f_m(X_m) - \int_{-\infty}^{+\infty} dx_i f_m(X_m) R_i(x_i), \quad (13)$$

where we assume that $R_i(x_i)$ is chosen in such a way that the integral term in the expression (13) exists. Finally, for each node i define the *centered partial energy function*

$E_i^g(X)$ as follows:

$$E_i^g(X) = - \sum_{m \in \mathcal{M}_i} \theta_m g_{im}(X_m). \quad (14)$$

Now we are ready to formulate the GISO-based objective function, which we refer to as Interaction Screening Objective for Distributions with Unbounded Support (ISODUS).

Definition 3 (Interaction Screening Estimator). *The ISODUS estimator is defined as a series of independent local optimization problems over p nodes:*

$$\hat{\Theta}_i^{IS} = \operatorname{argmin}_{\Theta_i} \langle \exp(-E_i^g(X)) R_i(x_i) \rangle, \quad (15)$$

where $E_i^g(X)$ is defined in (14).

Similarly to the post-processing step for the PL estimator, we use the geometric mean of model parameters estimated from different neighborhoods to produce the final estimate of Θ .

The original GISO introduced in (Vuffray et al., 2020) for discrete graphical models can be regarded as a special case of (15) where the MRD term $R_i(x_i)$ chosen as a uniform distribution over discrete alphabet of values that x_i can take. It is immediately apparent that for the uniform MRD the integral in (13) does not exist whenever f_m contains an even degree monomial in x_i , an issue that arises even for the simple case of normal distributions.

We propose the following choice of MRD with unbounded support which decays fast enough such that the ISODUS estimator (15) is properly defined:

$$R_i(x_i) = \frac{(s + \delta)}{2\Gamma\left(\frac{1}{s+\delta}\right)} \nu^{\frac{1}{s+\delta}} \exp(-\nu_i |x_i|^{s+\delta_i}), \quad (16)$$

where s_i is the maximum monomial order in the partial energy function (14), $\nu_i, \delta_i \geq 0$ are the user-defined hyper-parameters, Z_p^i is the normalization constant, and $\Gamma(\cdot)$ is the Gamma function.

Observe that since the basis functions f_m are polynomials the centering functions in (13) always exist, thus addressing the first issue with GISO. Also for any $\nu_i, \delta_i > 0$ (or for ν_i sufficiently large when $\delta_i = 0$) the term $-\nu_i |x_i|^{s_i+\delta_i}$ dominates all other monomials in the GISO exponent, leading to all its moments being finite.

For the sake of simplicity, in what follows we will choose $s_i = s$, where s is the maximum monomial order in the full energy function (2), and choose uniform values for the remaining hyper-parameters across all nodes, $\nu_i = \nu$ and $\delta_i = \delta$ for all $i \in V$. For the special choice in (16) and in the case of the energy function (2) expressed in the monomial basis, the centering functions in Eq. (13) can be computed

analytically. Since $R_i(x_i)$ is symmetric, all terms $f_m(X_m)$ where x_i appears at the odd power are already centered, i.e. for them $g_{im}(X_m) = f_m(X_m)$. So the only nontrivial terms are those that only contain x_i^k with k even (e.g. $k = 2$ or $k = 4$ in the example (4) above with up to fourth order interactions). For those terms, $g_{im}(X_m) = f_m(X_m) - c_i^{(k)} f_m(X_m)/x_i^k$, where the centering coefficients $c_i^{(k)}$ can be computed as follows:

$$c_i^{(k)} \equiv \int dx_i x_i^k R_i(x_i) = \frac{\nu^{-\frac{k}{s+\delta}} \Gamma\left(\frac{k+1}{s+\delta}\right)}{\Gamma\left(\frac{1}{s+\delta}\right)}. \quad (17)$$

For instance, for the terms of the type $f_{iijk}(x_i, x_j, x_k) = x_i^2 x_j x_k$, we get $g_{iijk}(x_i, x_j, x_k) = x_i^2 x_j x_k - c_i^{(2)} x_j x_k$, and for $f_{iiii}(x_i) = x_i^4$, we obtain $g_{iiii}(x_i) = x_i^4 - c_i^{(4)}$.

In experiments for both PL and ISODUS, we use the optimization software Ipopt (Wächter & Biegler, 2006) with tolerance 10^{-8} within the Julia/JuMP modeling framework for mathematical optimization (Dunning et al., 2017)¹.

3. Performance on Gaussian distributions

While the main advantages of ISODUS compared to PL become prominent for models with higher order interactions, we first consider the simple case of GGMs for ease of the computations needed for analyzing certain fundamental properties of ISODUS. We first study the estimation accuracy for different choices of the hyperparameters ν and γ and show that when these are chosen in an appropriate range, ISODUS can successfully recover GGMs. We then consider the so-called high dimensional setting for sparse GGMs and show that ISODUS with an ℓ_1 regularization attains the well-known $\log p$ scaling in sample complexity.

3.1. Properties of the ISODUS and choice of the MRD

We begin by studying the influence of hyperparameters δ and ν of the prior (16) on the performance of the estimator. For the Gaussian energy function (3), we have the maximum monomial order $s = 2$. We quantify the learning accuracy using the element-wise ℓ_1 reconstruction error $\epsilon \equiv \frac{1}{\dim(\Theta)} \|\hat{\Theta} - \Theta\|_1$, where \dim is the number of components of Θ . Here, we study a Gaussian distribution on 10 nodes, with a randomly-generated symmetric and positive semi-definite precision matrix.

In Figure 2, we sweep over a range of δ and ν for a single instance of the GGM learning problem on 10 nodes and plot the resulting reconstruction error. From Figure 2, it is apparent that in a region that encloses $(\delta = 0, \nu = 0)$ and which lies below a certain curve $\nu(\delta)$, ISODUS is not reg-

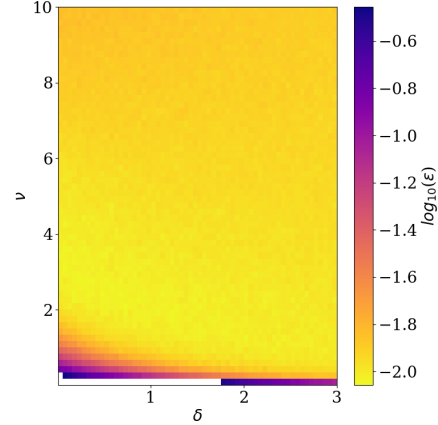


Figure 2. Element-wise reconstruction error ϵ as a function of hyperparameters δ and ν for a GGM learning problem on 10 nodes. Each axis has 50 steps, and each point has been averaged over 80 independent sets of 10^5 samples. The region in white is not shown as it results in high reconstruction errors.

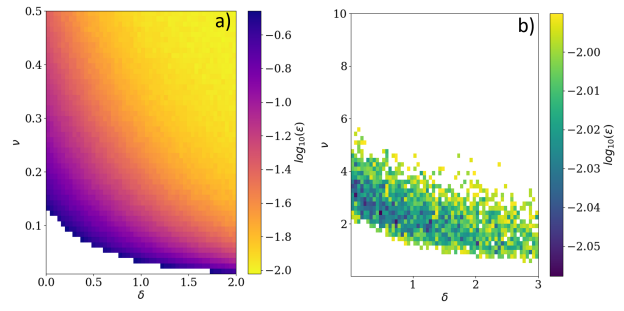


Figure 3. (a) Zoom on the line $\nu(\delta)$ that ensures a sufficient regularization of ISODUS. (b) The valley of optimal hyperparameters for the GGM learning problem, obtained by thresholding the heatmap in Figure 2 at the value $\log_{10} \epsilon = -1.99$. Both plots have a discretization of 50 steps along each axis, and each point has been averaged over 80 independent sets of 10^5 samples.

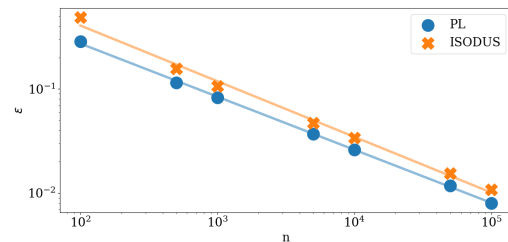


Figure 4. Scaling of the element-wise error in the reconstruction of model parameters with number of samples for PL and ISODUS for a GGM learning problem on 10 nodes. Each data point has been averaged over 25 independent sets of samples.

¹The code is available at <https://github.com/lanl-ansi/isodus/>.

ularized enough by the MRD and its reconstruction errors blow up dramatically. This region is magnified in Figure 3, (a). Above this line, the accuracy landscape looks like a valley with a weak dependence on the coefficient ν . Zooming into this valley, shown in Figure 3 (b), one realizes that as the prior becomes stronger with growing δ , almost any coefficient $\nu > 0$ leads to a small reconstruction error. In what follows, we fix the value of these hyperparameters to values in the intermediate range, $\delta = 2$ and $\nu = 2$, which ensure that the prior is not too strong, while the dependence on the optimal value of $\nu(\delta)$ remains relatively weak. For these regularization values, we show in Figure 4 that ISODUS enjoys the expected asymptotic scaling where the learning error decays with the number of samples as $\epsilon \propto 1/\sqrt{n}$, and exhibits similar absolute accuracy compared to the error obtained by the pseudolikelihood estimator.

3.2. Learning of sparse high-dimensional Gaussian graphical models

One important property of estimators for sparse graphical models in the high-dimensional regime consists in a weak dependence of the sample requirement on the dimension of the problem. This is characterized by the number of samples required for model selection n^* scaling only logarithmically with the dimension of the problem: $n^* \propto \log p$. Such high-dimensional estimators typically enforce sparsity via sparsity-promoting regularization. The convexity-preserving ℓ_1 regularization is a popular choice. In this section, we empirically verify that when supplemented with a sparsity regularizer, ISODUS exhibits a high-dimensional scaling $n^* \propto \log p$.

A typical setting in which such a scaling is conveniently derived is the structure learning problem, where the goal is to reconstruct the sparse support of the distribution. We adapt the same setting in our problem, as defined next.

Definition 4 (Structure Learning Problem). *Given n i.i.d. samples $\{X^{(k)}\}_{k=1,\dots,n}$ drawn from an unknown probability measure (1) with the sparse energy function (2), estimate the location of non-zero elements of Θ , i.e. the hyper-graph that defines the support of the distribution.*

The minimum number of samples for which the hyper-graph can be recovered with high probability is denoted by n^* . We design the following numerical experiment for checking the scaling of n^* as a function of problem size p . We consider a family of Gaussian graphical models of different sizes p supported on random regular graphs of degree $d = 3$. The precision matrix Θ has ones on the diagonal, and the strength of each non-zero edge is equal to $\kappa = 0.25$, which ensures that the resulting Θ is positive semi-definite. We generate i.i.d. samples for each family of distributions, and perform reconstructions of Θ using both estimators, PL and ISODUS, supplemented with sparsity-promoting ℓ_1

regularizers. For instance, Regularized ISODUS takes the following form:

$$\hat{\Theta}_i^{\text{IS}} = \underset{\Theta_i}{\operatorname{argmin}} \left(\langle \exp(-E_i^g(X) - \nu_i |x_i|^{s+\delta}) \rangle + \lambda_{\text{IS}} \sqrt{\frac{\log p}{n}} \sum_j |\theta_{ji}| \right), \quad (18)$$

and Regularized PL has a similar form with the respective regularization coefficient λ_{PL} . In order to fix the regularization coefficients λ_{IS} and λ_{PL} , we first run a preliminary study for $p = 50$ and sweep over sparsity hyperparameters to determine the optimal values for each estimator. Reconstruction error as a function of regularizer values is presented in Figure 5. For the remainder of the experiment, we fix the values of regularization coefficients to optimal values $\lambda_{\text{IS}} = 0.35$ and $\lambda_{\text{PL}} = 2.3$ obtained in this experiment.

Following this, we use regularized versions of PL and ISODUS to determine n^* for each p using the fixed values of sparsity hyperparameters. For each p , n^* is determined as follows. For a given number of samples n , once the symmetrized Θ is estimated, we threshold inferred pairwise coupling values at $\kappa/2 = 0.125$, i.e. only keeping $\theta_{ij} > \kappa/2$. The non-zero elements θ_{ij} in the precision matrix then define the reconstructed adjacency matrix of the graph, which can be compared to the underlying graph of the model. Let us define n^* as the smallest number of samples such that the graph is reconstructed correctly for 45 different and independent sets of samples in a row, which guarantees graph recovery with probability greater than 0.95 with at a statistical confidence of at least 90% (Lokhov et al., 2018). We use sequential search to determine n^* , increasing the search value by 25 samples if 45 trials are in a row are not successful, and decreasing by 10 if they are.

The resulting scaling of $n^*(p)$ is presented in Figure 6, where we further average over 5 independent graph realizations for each p . We see that both regularized PL and ISODUS show logarithmic scaling $n^* \propto \log p$ with the dimension. All existing theoretical analysis establishing the $\log p$ scaling heavily rely on Chernoff type concentration bounds that require all moments of the estimator to be finite. Our choice of MRD in (16) ensures finiteness of all moments and the empirical $\log p$ scaling observed in this section supports this choice.

4. Tests on general non-Gaussian exponential family distributions

In this section, we illustrate the advantages of ISODUS for learning general non-Gaussian distributions compared to PL. First, we consider a one-dimensional exponential family distribution with higher-order interactions, and compare ISODUS and PL both in terms of their accuracy, as well

as in computational complexity. This family represents the simplest non-Gaussian case where we have to resort to numerical integration for computing the normalization factor Z_i that enters in the PL estimator. Finally, we illustrate that ISODUS retains its desirable computational and sample scaling properties on more complex multivariate distribution with multi-body interactions.

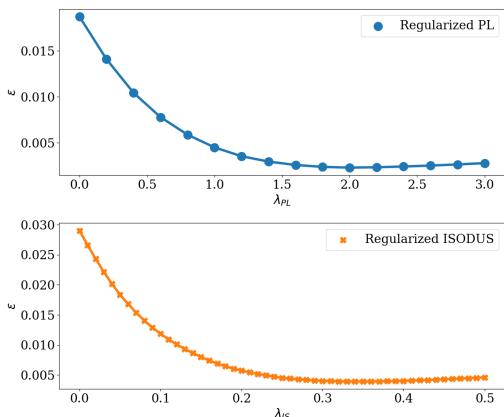


Figure 5. Sweep over λ_{IS} and λ_{PL} hyperparameters for regularized versions of PL and ISODUS for the GGM with $p = 50$ nodes. The minima of the reconstruction errors are obtained for $\lambda_{IS} = 0.35$ and $\lambda_{PL} = 2.3$.

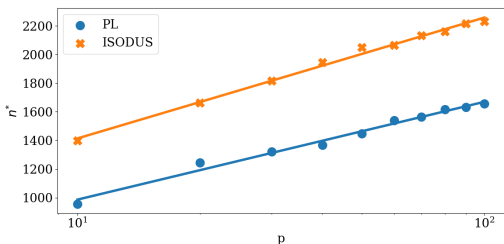


Figure 6. Scaling of required number of samples n^* for structure learning problem in GGMs on random regular graphs with degree $d = 3$ as a function of problem size p using the optimal values of the sparsity-promoting regularization coefficients. Each data point is averaged over 5 independent graph realizations of size p . For each model, n^* is determined as the minimum number of samples that leads to a successful graph recovery for 45 independent sets of samples. Both regularized PL and ISODUS estimators show logarithmic scaling $n^* \propto \log p$, desirable for the high-dimensional structure learning problem.

4.1. One-dimensional non-Gaussian distribution

As an example of a one-dimensional non-Gaussian distribution, we take an exponential family (1) with the energy function $E(X) = -x^2 - 0.5x^3 - 2x^4$. Unlike for GGMs, sample generation for models with higher-order moments is non-trivial. To ensure high-quality independent and identi-

cally distributed samples, we employ brute-force sampling using fine discretization with 5000 bins.

As a first experiment, we compare the accuracies of ISODUS and PL for this test case. The results on the learning error are presented in Figure 7. We used a relative tolerance of factor 10^{-7} in the evaluation of the normalization factor Z at each step of the optimization procedure. Both algorithms demonstrate similar accuracy, and asymptotically normal error decay with the number of samples.

As the next test, we check the pure computational run-time of both algorithms on this instance as a function of the number of samples. The comparison of run-times is presented in Figure 8. The difference in running time is explained by the additional overhead of numerical estimation of the local normalization factors required during the PL optimization subroutine. This numerical estimation up to a given precision has been performed using the QuadGK.jl library based on the adaptive Gauss-Kronrod quadrature (QuadGK.jl, 2020). It is natural to assume that the complexity of adaptive numerical integration up to a prescribed tolerance may increase with the complexity of the integrand. To test this hypothesis, we ran a comparison of run-times of both algorithms for learning one-dimensional distributions with energy functions of increasing monomial order L . The ratio of run-times of PL and ISODUS for a fixed number of samples $n = 100$ is plotted in Figure 9 for the models with the energy function $E(X) = -\sum_{l=2}^L \alpha_l x^l$ where α_l have been randomly selected from $[0, 1]$. We see that the computational overhead of PL may significantly increase with the complexity of the model.

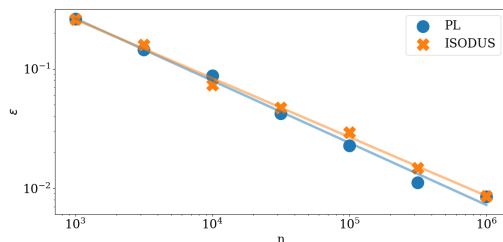


Figure 7. Scaling of the element-wise error in reconstruction of model parameters with the number of samples for PL and ISODUS for a test one-dimensional distribution with the energy function of degree 4. Each point has been averaged over 45 independent sets of samples.

4.2. Multivariate exponential family with higher-order interactions

Results on one-dimensional distributions demonstrate ISODUS shows similar reconstruction results in terms of accuracy when compared to the baseline PL method, but benefits from a much lower computational complexity. Here, we il-

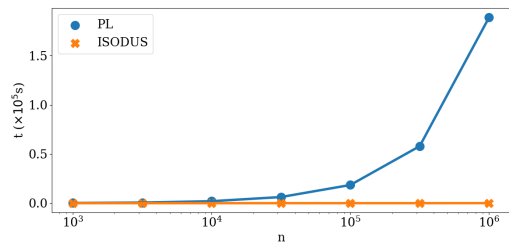


Figure 8. Comparison of run-times of PL and ISODUS estimators in the case of one dimensional non-Gaussian distribution as a function of number of samples. PL run-time includes a computational overhead due to the necessity of numerical estimation of local normalization factors.

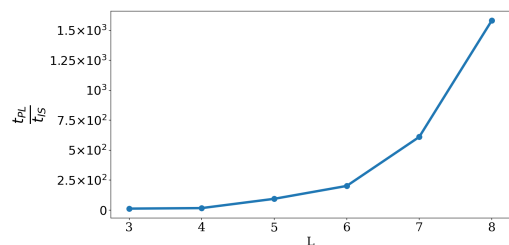


Figure 9. Dependence of the ratio of running times of PL and ISODUS as a function of the maximum degree of the polynomial energy function L for one-dimensional non-Gaussian distributions.

illustrate the scalings of ISODUS on a four-dimensional problem with an energy function that contains higher-order interactions up to order 4. To ensure the quality of the samples remains high, we aim to maintain the same discretization level (5000 points per dimension) in this problem as well, which leads to an intractable resolution for general four-dimensional distributions. We chose to construct a pseudo four-dimensional distribution, which factorizes over two pairs of variables. Hence, i.i.d. samples from the ground-truth distribution could be constructed from a combination of two independent 4-body distributions over two variables each. The ISODUS estimator was not fed with this information, and had to learn the structure of the model from the provided four-dimensional samples. The scaling of the reconstruction error as a function of number of samples is given in the Figure 10. PL’s run-time renders the algorithm essentially intractable for this problem. We also verify that as expected, the run-time of ISODUS is linear as a function of number of samples, as shown in Figure 11.

5. Conclusion

In this paper, we introduced a new estimator, ISODUS, adapted from the Interaction Screening method to the challenging case of general exponential family distributions with unbounded support. We studied the properties of this

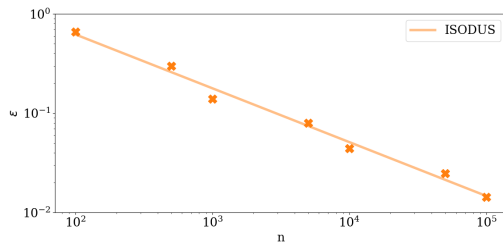


Figure 10. Scaling of the reconstruction error of ISODUS as a function of number of samples on a four-dimensional four-body distribution. ISODUS shows an expected scaling $\epsilon \propto 1/\sqrt{n}$. Each point has been averaged over 45 independent sets of samples.

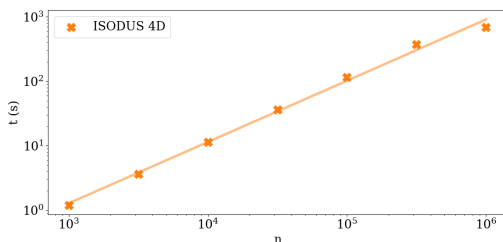


Figure 11. Linear run-time scaling of ISODUS with the number of samples for a four-dimensional four-body distribution. Each point has been averaged over 45 independent sets of samples.

estimator for high-order distributions as well as for Gaussians, and established empirically that it poses an error dependence with respect to the number of samples similar to the pseudolikelihood approach. However, ISODUS avoids computing local normalization factors that makes the pseudolikelihood algorithm computationally prohibitive. This makes ISODUS the estimator of choice for learning continuous non-Gaussian graphical models.

We have shown how the inclusion of sparsity regularization allows one to recover the high-dimensional scaling $n^* \propto \log p$ for structure learning and parameter estimation problems. This sparsity regularization can be extended to factor graphs to reduce the sample requirements for sparse problems. A natural follow-on would consist of complementing the empirical study presented in this paper with a theoretical analysis to establish rigorous guarantees on the sample complexity of regularized ISODUS estimator.

We have focused on distributions with high-order terms in the form of monomials which are especially important in applications where non-Gaussian statistics are relevant. However, it would be interesting to study ISODUS for other families of sufficient statistics, or even for implicit parametrizations of the energy function such as Neural Networks introduced recently for discrete graphical models (Abhijith J. et al., 2020).

Acknowledgements

We acknowledge support from the Laboratory Directed Research and Development program of Los Alamos National Laboratory under project numbers 20190059DR, 20200121ER, and 20210078DR.

References

- Abhijith J., Likhov, A., Misra, S., and Vuffray, M. Learning of discrete graphical models with neural networks. In *Advances in Neural Information Processing Systems (NeurIPS)* 33. 2020.
- Anandkumar, A., Tan, V. Y., Huang, F., and Willsky, A. S. High-dimensional gaussian graphical model selection: Walk summability and local separation criterion. *Journal of Machine Learning Research*, 13(Aug):2293–2337, 2012.
- Banfield, J. D. and Raftery, A. E. Model-based gaussian and non-gaussian clustering. *Biometrics*, pp. 803–821, 1993.
- Besag, J. Statistical analysis of non-lattice data. *Journal of the Royal Statistical Society: Series D (The Statistician)*, 24(3):179–195, 1975.
- Bouguila, N., Ziou, D., and Vaillancourt, J. Unsupervised learning of a finite mixture model based on the dirichlet distribution and its application. *IEEE Transactions on Image Processing*, 13(11):1533–1543, 2004.
- Cai, T., Liu, W., and Luo, X. A constrained ℓ_1 minimization approach to sparse precision matrix estimation. *Journal of the American Statistical Association*, 106(494):594–607, 2011.
- Cai, T. T., Liu, W., and Zhou, H. H. Estimating sparse precision matrix: Optimal rates of convergence and adaptive estimation. *The Annals of Statistics*, 44(2):455–488, 2016.
- d’Aspremont, A., Banerjee, O., and Ghaoui, L. E. First-order methods for sparse covariance selection. *SIAM Journal on Matrix Analysis and Applications*, 30(1):56–66, 2008.
- Dobra, A., Lenkoski, A., et al. Copula gaussian graphical models and their application to modeling functional disability data. *The Annals of Applied Statistics*, 5(2A): 969–993, 2011.
- Dunning, I., Huchette, J., and Lubin, M. Jump: A modeling language for mathematical optimization. *SIAM Review*, 59(2):295–320, 2017. doi: 10.1137/15M1020575.
- Ghosh, S. K., Cherstvy, A. G., Grebenkov, D. S., and Metzler, R. Anomalous, non-gaussian tracer diffusion in crowded two-dimensional environments. *New Journal of Physics*, 18(1):013027, 2016.
- Goel, S., Kane, D. M., and Klivans, A. R. Learning using models with independent failures. In *Conference on Learning Theory*, pp. 1449–1469. PMLR, 2019.
- Hoffman, M. D., Blei, D. M., and Cook, P. R. Bayesian nonparametric matrix factorization for recorded music. In *Proceedings of the 27th International Conference on International Conference on Machine Learning, ICML’10*, pp. 439–446, Madison, WI, USA, 2010. Omnipress. ISBN 9781605589077.
- Jakeman, E. and Tough, R. Non-gaussian models for the statistics of scattered waves. *Advances in Physics*, 37(5): 471–529, 1988.
- Ji, Y., Wu, C., Liu, P., Wang, J., and Coombes, K. R. Applications of beta-mixture models in bioinformatics. *Bioinformatics*, 21(9):2118–2122, 2005.
- Kelner, J., Koehler, F., Meka, R., and Moitra, A. Learning some popular gaussian graphical models without condition number bounds. In *Advances in Neural Information Processing Systems (NeurIPS)* 33. 2020.
- Klivans, A. and Meka, R. Learning graphical models using multiplicative weights. In *2017 IEEE 58th Annual Symposium on Foundations of Computer Science (FOCS)*, pp. 343–354, Oct 2017.
- Kogut, A., Banday, A., Bennett, C., Górski, K., Hinshaw, G., Smoot, G., and Wright, E. Tests for non-gaussian statistics in the dmr four-year sky maps. *The Astrophysical Journal Letters*, 464(1):L29, 1996.
- Koopman, B. O. On distributions admitting a sufficient statistic. *Transactions of the American Mathematical Society*, 39(3):399–409, 1936.
- Koutis, I. On the hardness of approximate multivariate integration. In *Approximation, Randomization, and Combinatorial Optimization.. Algorithms and Techniques*, pp. 122–128. Springer, 2003.
- Lafferty, J., Liu, H., Wasserman, L., et al. Sparse non-parametric graphical models. *Statistical Science*, 27(4): 519–537, 2012.
- Lee, J. D. and Hastie, T. J. Learning the structure of mixed graphical models. *Journal of Computational and Graphical Statistics*, 24(1):230–253, 2015.
- Li, Y. and Meneveau, C. Origin of non-gaussian statistics in hydrodynamic turbulence. *Physical review letters*, 95 (16):164502, 2005.

- Liu, H., Lafferty, J., and Wasserman, L. The nonparanormal: Semiparametric estimation of high dimensional undirected graphs. *Journal of Machine Learning Research*, 10(Oct):2295–2328, 2009.
- Liu, H., Han, F., Yuan, M., Lafferty, J., Wasserman, L., et al. High-dimensional semiparametric gaussian copula graphical models. *The Annals of Statistics*, 40(4):2293–2326, 2012.
- Lokhov, A. Y., Vuffray, M., Misra, S., and Chertkov, M. Optimal structure and parameter learning of Ising models. *Science Advances*, 4(3):e1700791, 2018.
- Ma, Z. *Non-Gaussian statistical models and their applications*. PhD thesis, KTH Royal Institute of Technology, 2011.
- Meinshausen, N. and Bühlmann, P. High-dimensional graphs and variable selection with the lasso. *The annals of statistics*, pp. 1436–1462, 2006.
- Misra, S., Vuffray, M., and Lokhov, A. Y. Information theoretic optimal learning of gaussian graphical models. In *Conference on Learning Theory*, pp. 2888–2909. PMLR, 2020.
- Morrison, R., Baptista, R., and Marzouk, Y. Beyond normality: Learning sparse probabilistic graphical models in the non-gaussian setting. In *Advances in Neural Information Processing Systems*, pp. 2359–2369, 2017.
- Perron, M. and Sura, P. Climatology of non-gaussian atmospheric statistics. *Journal of climate*, 26(3):1063–1083, 2013.
- QuadGK.jl. <https://github.com/JuliaMath/QuadGK.jl>, 2020.
- Ravikumar, P., Raskutti, G., Wainwright, M. J., and Yu, B. Model selection in gaussian graphical models: High-dimensional consistency of ℓ_1 -regularized MLE. In *Advances in Neural Information Processing Systems 21*, pp. 1329–1336, 2009.
- Ravikumar, P., Wainwright, M. J., Lafferty, J. D., et al. High-dimensional Ising model selection using ℓ_1 -regularized logistic regression. *The Annals of Statistics*, 38(3):1287–1319, 2010.
- Sengupta, A., Cressie, N., Kahn, B. H., and Frey, R. Predictive inference for big, spatial, non-gaussian data: Modis cloud data and its change-of-support. *Australian & New Zealand Journal of Statistics*, 58(1):15–45, 2016.
- Shah, A., Shah, D., and Wornell, G. W. On learning continuous pairwise markov random fields. *arXiv preprint arXiv:2010.15031*, 2020.
- Suggala, A. S., Kolar, M., and Ravikumar, P. The exp-orcist: Nonparametric graphical models via conditional exponential densities. *Advances in neural information processing systems*, 30:4446, 2017.
- Sun, S., Kolar, M., and Xu, J. Learning structured densities via infinite dimensional exponential families. In *Proceedings of the 28th International Conference on Neural Information Processing Systems-Volume 2*, pp. 2287–2295, 2015.
- Tansey, W., Padilla, O. H. M., Suggala, A. S., and Ravikumar, P. Vector-space markov random fields via exponential families. In *International Conference on Machine Learning*, pp. 684–692. PMLR, 2015.
- Tibshirani, R. Regression shrinkage and selection via the lasso. *Journal of the Royal Statistical Society. Series B (Methodological)*, pp. 267–288, 1996.
- Titterton, D. M., Smith, A. F., and Makov, U. E. *Statistical analysis of finite mixture distributions*. Wiley, 1985.
- Vuffray, M., Misra, S., Lokhov, A., and Chertkov, M. Interaction screening: Efficient and sample-optimal learning of Ising models. In Lee, D. D., Sugiyama, M., Luxburg, U. V., Guyon, I., and Garnett, R. (eds.), *Advances in Neural Information Processing Systems 29*, pp. 2595–2603. Curran Associates, Inc., 2016.
- Vuffray, M., Misra, S., and Lokhov, A. Efficient learning of discrete graphical models. In *Advances in Neural Information Processing Systems (NeurIPS) 33*. 2020.
- Wächter, A. and Biegler, L. T. On the implementation of an interior-point filter line-search algorithm for large-scale nonlinear programming. *Mathematical programming*, 106(1):25–57, 2006.
- Wainwright, M. J., Jordan, M. I., et al. Graphical models, exponential families, and variational inference. *Foundations and Trends® in Machine Learning*, 1(1–2):1–305, 2008.
- Xue, L., Zou, H., et al. Regularized rank-based estimation of high-dimensional nonparanormal graphical models. *The Annals of Statistics*, 40(5):2541–2571, 2012.
- Yang, E., Ravikumar, P., Allen, G. I., and Liu, Z. Graphical models via univariate exponential family distributions. *The Journal of Machine Learning Research*, 16(1):3813–3847, 2015.
- Yang, Z., Ning, Y., and Liu, H. On semiparametric exponential family graphical models. *The Journal of Machine Learning Research*, 19(1):2314–2372, 2018.

Yuan, M. and Lin, Y. Model selection and estimation in the gaussian graphical model. *Biometrika*, pp. 19–35, 2007.

Yuan, X.-T., Li, P., Zhang, T., Liu, Q., and Liu, G. Learning additive exponential family graphical models via $\ell_{2,1}$ -norm regularized m-estimation. In *NIPS*, 2016.